

Catalytic subunits *atp α* and *atp β* from the Pacific white shrimp *Litopenaeus vannamei* F₀F₁ ATP-synthase complex: cDNA sequences, phylogenies, and mRNA quantification during hypoxia

Oliviert Martinez-Cruz · Fernando Garcia-Carreño ·
Arlett Robles-Romo · Alejandro Varela-Romero ·
Adriana Muhlia-Almazan

Received: 13 August 2010 / Accepted: 8 December 2010 / Published online: 8 March 2011
© Springer Science+Business Media, LLC 2011

Abstract In the mitochondrial F₀F₁ ATP-synthase/ATPase complex, subunits α and β are part of the extrinsic portion that catalyses ATP synthesis. Since there are no reports about genes and proteins from these subunits in crustaceans, we analyzed the cDNA sequences of both subunits in the whiteleg shrimp *Litopenaeus vannamei* and their phylogenetic relationships. We also investigated the effect of hypoxia on shrimp by measuring changes in the mRNA amounts of *atp α* and *atp β* . Our results confirmed highly conserved regions for both subunits and underlined unique features among others. The ATP β deduced protein of shrimp was less conserved in size and sequence than ATP α . The relative mRNA amounts of *atp α* and *atp β* changed in shrimp pleopods; hypoxia at 1.5 mg/L caused an increase in *atp β* transcripts and a subsequent decrease when shrimp were re-oxygenated. Results confirm that changes in the mRNAs of the ATP-synthase subunits are

part of the mechanisms allowing shrimp to deal with the metabolic adjustment displayed to tolerate hypoxia.

Keywords *atp α* subunit · *atp β* subunit · F₀F₁ATP synthase · Hypoxia · Shrimp

Introduction

The mitochondrial F₀F₁ ATP-synthase complex is a multimeric enzyme that catalyzes the synthesis of adenosine triphosphate (ATP) from adenosine diphosphate (ADP) and inorganic phosphate (P_i). This catalytic process is triggered by the electrochemical gradient of protons generated along the electron transport chain in the mitochondrion (Pedersen 2007). This enzyme synthesizes 95% of the ATP molecules in cells, and its function is closely related to the presence of oxygen that takes electrons yielded by this electron transport chain (Alberts et al. 2008). The F₀F₁ ATP synthase is formed by two major components, a catalytic headpiece F₁, and a base-piece/stalk membrane-embedded F₀. Minor components involve subunits which are encoded in the nucleus and in the mitochondrion genome (Walker et al. 1991). As other nucleus-encoded proteins, the ATP-synthase subunits possess a short N-terminal sequence that signals their importation into the mitochondrion (Schatz and Butow 1983). The catalytic building block of F₁ is formed by a subcomplex of 3 α and 3 β subunits (Abrahams et al. 1994; Boyer 1997); all of them are encoded in the nuclear genome, translated in the cytoplasm, and imported into the mitochondrion as pre-proteins (Walker and Runswick 1983; Breen 1988).

O. Martinez-Cruz · A. Muhlia-Almazan (✉)
Molecular Biology Laboratory,
Centro de Investigacion en Alimentacion y Desarrollo (CIAD),
Carretera a La Victoria Km 0.6, P.O. Box. 1735, Hermosillo,
Sonora 83000, Mexico
e-mail: amuhlia@ciad.mx

F. Garcia-Carreño · A. Robles-Romo
Biochemistry Laboratory,
Centro de Investigaciones Biologicas del Noroeste (CIBNOR),
Mar Bermejo 195, Col. Playa Palo de Santa Rita, P.O. Box 128,
La Paz, Baja California Sur 23090, Mexico

A. Varela-Romero
Departamento de Investigaciones Cientificas y Tecnologicas
de la Universidad de Sonora,
P.O. Box 1819, Blvd. Luis D. Colosio s/n,
Hermosillo, Sonora 83000, Mexico

In eukaryotic organisms the main regulatory mechanisms that act in the oxidative phosphorylation system (OXPHOS) include substrate availability (NADH, ADP), membrane potential, allosteric regulation, reversible phosphorylation, and the expression of tissue-specific isoforms (Hüttemann et al. 2008). In the ATP-synthase complex, subunits α and β have been deeply studied in animal and plant models because they directly participate during catalysis and the existence of various isoforms from both genes have been confirmed in some species to participate during enzyme regulation in a tissue-function-specific manner (Kataoka and Biswas 1991; Lalanne et al. 1998; Hoskins et al. 2007).

Studies on the mitochondrial F_0F_1 ATP synthase from invertebrate species are scarce, especially in crustaceans. One complete mRNA sequence of *atp β* in the crayfish *Pacifastacus leniusculus* has been reported in the GenBank (Accession Number DQ874396), and few partial sequences of *atp α* from crustaceans have been found as ESTs (expressed sequences tags) in the same data base.

Marine crustaceans are commonly exposed to fluctuating dissolved oxygen concentrations (OC) in water along their life cycle. Hypoxia is the condition that results from low oxygen concentrations in marine coastal waters affecting organisms fitness and survival (Wu et al. 2002). The biological responses of crustaceans to hypoxia include a metabolic reorganization, the switch to anaerobic metabolism, avoidance behaviour, increase in the frequency of ventilatory movements and metabolic rate depression (Morris et al. 2005).

In this study we analyzed, for the first time, the *atp α* and *atp β* subunits of the mitochondrial F_0F_1 ATP-synthase complex from the Pacific white shrimp *Litopenaeus vannamei* to obtain basic information that includes the description of the complementary DNA (cDNA) sequences, phylogenetic relationships, the steady-state mRNA detection of both subunits in gills and pleopods, and the effect of hypoxia on the expression of the codifying genes to obtain new insights related to the organization of ATP synthesis in this marine invertebrate.

Materials and methods

Animals and bioassays

A bioassay was conducted in the laboratory with adult *L. vannamei* shrimp weighing 30 ± 1 g. Shrimp were acclimated to laboratory conditions for 8 days in marine water at 28 °C, 35 ppt salinity, constant aeration at 6 mg/L OC, and commercial food was supplied twice a day. After acclimation, five shrimp were decapitated and gills were dissected and submerged in 250 μ L of TRIzol reagent

(Invitrogen, Carlsbad, CA) for total RNA isolation and cDNA sequencing purposes.

A preliminary assay was conducted to determine the gradually decreasing of dissolved OC in water, as it occurs in coastal waters or aquaculture ponds, by removing air-stones from an experimental 1,000 L tank containing 30 shrimp at a constant water volume. Dissolved oxygen concentration in water was continuously measured with a digital oxymeter until water reached the lowest OC value recorded (1.5 mg/L), which remained constant.

The hypoxia assay was conducted using 270 adult shrimp that were randomly distributed in nine 1,000 L tanks ($n=30$ each) and kept under normoxia (6 mg/L). After acclimation, all shrimp were starved for 24 h, then three tanks were kept at normoxia as the control group and three shrimp were collected from each tank. The air supply was stopped in the six remaining tanks to induce hypoxia. Three shrimp were collected from each tank when OC decreased to 4.0, 2.0, and 1.5 mg/L with intervals of 4–5 h between samplings. Then, the six tanks were gradually re-oxygenated by placing air-stones in each tank, and when the OC reached 7 mg/L, three last shrimp were collected.

Molting stages were previously determined in all shrimp according to the setogenesis phase (formation of new seta in uropods) (Chan et al. 1988). All experimental organisms included in the assay were at intermolt stage. Once collected, shrimp were decapitated and gills and pleopods were dissected and stored in TRIzol reagent (Invitrogen, Carlsbad, CA) at -80 °C until used.

Each shrimp was weighed and 400 μ L of hemolymph were extracted from the base of the fifth pereopod with a 1-mL syringe containing two volumes of pre-cooled shrimp anticoagulant solution containing 300 mM NaCl, 10 mM KCl, 10 mM HEPES, 10 mM EDTA at pH 7.3 (Vargas-Albores et al. 1993). Each hemolymph sample was centrifuged at $7,000 \times g$ for 10 min at 4 °C. Plasma and hemocytes were separated, and both were stored at -80 °C until used. Glucose and lactate concentrations were measured with commercial kits for medical diagnosis (RANDOX, GL2614 and LC2389, Antrim, UK) as indicators of the hypoxia effect on shrimp plasma.

Atp α and *atp β* cDNA sequencing

Total RNA was isolated from gills using TRIzol reagent following the manufacturer instructions. Five μ g of total RNA were used to synthesize cDNA using the GeneRacer kit as specified by the manufacturer (Invitrogen, Carlsbad CA). The cDNA was used as a template for PCR amplifications. Various specific oligonucleotides were designed for each subunit based on mRNA and ESTs sequences available at the GenBank for *atp α* (BF024234, FE066413, and FE100354, Gross et al. 2001), and for *atp β*

(DQ874396) from crustacean and other invertebrate species (Table 1).

PCR amplifications were carried out to obtain the full cDNA sequence of both subunits. A BD Advantage 2 polymerase mix (BD Biosciences Clontech, Palo Alto, CA) was used in a total volume reaction of 25 μ L that included 1 μ L of cDNA (equivalent to 250 ng total RNA), specific forward or reverse oligonucleotides (Table 1), and one of the forward or reverse oligonucleotides provided in the RACE kit to amplify 5'- and 3'- ends. A thermocycler (DNA Engine, BioRad, Hercules, CA) was used at the following conditions: 3 min at 94 °C (1 cycle); 30 s at 94 °C, 30 s at 60–62 °C, and 1 min at 68 °C for (30 cycles). The resulting PCR products were analyzed in 1.5% agarose gels (Sambrook and Russell 2001) and stained with SYBR Safe (Invitrogen, Carlsbad, CA). PCR products were purified and cloned using a TOPO TA cloning kit (Invitrogen, Carlsbad, CA) and sequenced at Macrogen Inc. (Seoul, Korea).

The predicted amino acid sequence of both subunits was obtained in the web site <http://au.expasy.org/tools/>. Sequence analyses were performed using Blast (N, X and P), and Clustal W algorithms (Thompson et al. 1994; Altschul et al. 1997). The Mitoprot software was used to predict and analyze the mitochondrial protein sequences (<http://ihg2.helmholtz-muenchen.de/ihg/mitoprot.html>; Claros and Vincens 1995).

Phylogenetic analysis

Phylogenetic relationships of ATP α and ATP β were determined including both complete sequences from *L. vannamei* (ATP α GQ848643 and ATP β GQ848644); we included available sequences of ATP α : *Drosophila melanogaster* (NP_726243); *Drosophila yakuba* (XP_002092136); *Bombix mori* (NP_001040233); *Pediculus humanus corporis* (EEB14270); *Aedes aegypti* (XP_001655906); *Mus musculus*

(NP_031531); *Xenopus laevis* (NP_001081246); *Xenopus tropicalis* (NP_001025610); *Danio rerio* (NP_001070823); *Salmo salar* (ACN10935); *Caenorhabditis elegans* (NP_001021526); *Anopheles gambiae* (XP_314018); *Ixodes scapularis* (EEC16574); *Bos taurus* (NP_777109); *Homo sapiens* (NP_004037); *Escherichia coli* (AAA24735); *Pinctada fucata* (ABJ51956); *Gallus gallus* (NP989617); *Saccharomyces cerevisiae* (NP_009453), and ATP β : *D. melanogaster* (CAA50332); *D. yakuba* (XP_002099634); *Drosophila pseudoobscura pseudoobscura* (EAL29273); *B. mori* (NP_001040450); *P. humanus corporis* (EEB19469); *A. aegypti* (XP001656737); *Culex quinquefasciatus* (XP_001847944); *M. musculus* (AAB86421); *B. taurus* (NP_786990); *H. sapiens* (AAA51808); *X. laevis* (NP_001080126); *X. tropicalis* (NP_001001256); *D. rerio* (NP_001019600); *C. elegans* (NP_498111); *I. scapularis* (EEC17118); *Pacifastacus leniusculus* (ABI34071); *P. fucata* (ABC86835); *S. cerevisiae* (NP_012655); and *E. coli* (AAA24737).

All sequences were aligned using Clustal W algorithm (Thompson et al. 1994) and construction of phylogenetic hypothesis from the dataset was done using the neighbor joining (NJ), and maximum parsimony (MP) methods. Both, nucleotide and amino acid sequences were used during constructions, and as the same topology was observed for both criteria, only the amino acid trees were analyzed.

Atp α and *atp β* mRNA quantification by qRT-PCR

Dissected gills and pleopods from experimental groups were homogenized using TRIzol (Invitrogen, Carlsbad, CA, USA) as specified by the manufacturer. Total RNA concentration was evaluated spectrophotometrically (260/280 nm) and RNA integrity was analyzed in a 1.5% formaldehyde-agarose gel electrophoresis (Sambrook and Russell 2001). DNA was removed from RNA samples by

Table 1 Specific oligonucleotides used for PCR amplification of shrimp F₁ ATP-synthase subunits *atp α* , *atp β* , and *L8* genes

Gene	Oligonucleotide name	Sequence (5'-3')	cDNA positions (nt)
<i>Atpα</i>	ATPAFw1CB	CTCTTCTTTGGCTCGTCAC	27–45
<i>Atpα</i>	ATPAFw2CB	ACAACATGGCTCTCGTCTCC	–5–15
<i>Atpα</i>	ATPAFw3CB	TCAACTTGGAGCCCGATAAC	311–330
<i>Atpα</i>	ATPARv1CB	CCATAGACACGGGCAATACC	248–229
<i>Atpα</i>	ATPARv5	GGAGCAGCATCAGAGGCAGTGGCAGAC	842–816
<i>Atpα</i>	ATPARv9CB	TTAGCAATCTACCCTAGCCCAC	1733–1711
<i>Atpβ</i>	ATPBFw1CB	GGTGCTGGTGTAGGAAAGAC	613–632
<i>Atpβ</i>	ATPBFw5	ATCATGTTGGGAGCTGCACAG	–3–18
<i>Atpβ</i>	ATPBFw6	GGTAATGCTGTCGTTGATACT	358–378
<i>Atpβ</i>	ATPBRv1CB	GGCTCGTTCATCTGACCGTA	818–799
<i>Atpβ</i>	ATPBRv6	ATGCGGCCAAGAGTACCAGGACCAACAG	423–399
<i>L8</i>	L8Fw3	TAGGCAATGTCATCCCCATT	223–242
<i>L8</i>	L8Rv3	TCCTGAAGGAAGCTTTACACG	320–300

digestion with DNase I (Roche, Indianapolis, IN) according to manufacturer instructions. To evaluate mRNA concentration from shrimp samples, 4 µg of total RNA were reverse transcribed using the Superscript III first strand synthesis system (Invitrogen, Carlsbad, CA,) and oligo (dT) oligonucleotide.

We assessed the steady-state mRNA amount of *atpα* and *atpβ* using an iQ5 multicolor real-time PCR detection system (BioRad, Hercules, CA). Specific oligonucleotide pairs were used to amplify *atpα* (ATPAFw1 and ATPARv1), and *atpβ* fragments (ATPBFW1 and ATPBRv1). The ribosomal protein *L8* (DQ316258) was used as an internal control gene to normalize *atpα* and *atpβ* expression (Table 1). Real time PCR amplifications were done in duplicates. Total volume reactions of 25 µL included 12.5 µL of 2X iQ SYBR Green supermix (BioRad, Hercules, CA), 1 µL (20 µM) of the corresponding forward and reverse oligonucleotides, cDNA synthesized from 250 ng of total RNA from each individual sample and water. PCR conditions were: 95 °C for 5 min followed by 40 cycles at 95 °C for 30 s, 62 °C for 1 min, 68 °C for 55 s with a final melting curve program from 60 °C to 95 °C increasing 0.3 °C each 20 s. Fluorescence readings were taken at 68 °C after each amplification cycle.

To calculate changes in mRNA concentration the $2^{-\Delta\Delta CT}$ method reported by Livak and Schmittgen (2001) was used. The calculation is based on the C_T value of each sample during PCR amplification and the formula $2^{-((CT_{atp\alpha} - CTL8)_{hypoxia} - (CT_{atp\alpha} - CTL8)_{normoxia})}$. Results are expressed as the fold change in mRNA steady-state amount of the target gene normalized to the *L8* ribosomal protein and relative to normoxia conditions (6 mg/L). Data obtained were analyzed by one way ANOVA and for post hoc analysis the Tukey test was used. Statistical significance was considered when $p < 0.05$. Analyses were performed using Statistica v 8.0 software.

Results

Atpα cDNA sequence

Two PCR fragments of expected size were amplified from gills cDNA using oligonucleotide pairs ATPAFw2/ATPARv5 and ATPAFw3/ATPRv9, the resulting fragments overlapped and produced a confirmed complete cDNA sequence including the coding region with an open reading frame which comprises 1,653 base pairs (bp) containing putative start (ATG) and stop (TAA) codons (GQ848643). This cDNA sequence comprises in the 5'-end, a 138 bp region that codes a putative signal peptide (46 residues), the mature protein of 1,515 bp at positions 139–1,653, and finally the 3'-UTR is 465 bp long including a polyadenylation signal and the poly A tail (Fig. 1). The *atpα* cDNA sequence

of *L. vannamei* without the signal peptide shows high identity with those of insect species as the yellow fever mosquito *A. aegypti* (83%, DQ440037; Ribeiro et al. 2007), the fruit fly *D. melanogaster* (82%, Y07894), and the silkworm *B. mori* (81%, DQ311340).

The deduced amino acid sequence of the pre-protein ATPα is 550 residues long, with a predicted molecular weight of 59.23 kDa (Figs. 1 and 2). The putative signal peptide of 46 residues in the N-terminal region, which is supposed to be the mitochondrial import sequence, contains 6 positively charged amino acids and no negatively charged ones. The ATPα mature protein is 504 amino acids long with a predicted molecular weight of 54.49 kDa, and an isoelectric point of 7.80.

Three conserved domains were identified in shrimp ATPα subunit, (i) the ATP-synt_ab_N domain at positions 66–132, (ii) the ATP-synt_ab domain (or nucleotide binding domain) at positions 188–412, which also includes the Walker A motif at positions 209–216 (GDRQTGKT), and the Walker B motif at positions 305–309 (LIYD), both of them commonly observed in those proteins including nucleotide binding sites, and finally, (iii) the ATP-synt_ab_C domain at positions 424–528 (Fig. 2; Walker et al. 1982).

Fifteen predicted amino acids which help to bind ATP (binding sites) were detected along the ATP-synt_ab domain at positions 211, 215, 216, 217, 243, 248, 309, 310, 313, 368, 384, 397, 402, 403, and 413 most of them highly conserved among species, and thirty four predicted sites of ATPα were located at the interface with ATPβ subunit at positions 155–156, 172–173, 175–176, 179, 181, 211–212, 249–252, 254–255, 258, 319–320, 326–328, 330–331, 336, 340, 343, 347, 384, 387, 398–399, 402, and 413 (Marchler-Bauer et al. 2009; Fig. 2). Some amino acid substitutions were detected in the *L. vannamei* protein sequence: T50, S63, N64, R123, A142, G163, G164, and L165, and some others were identified as invertebrate species shared residues: A60, P61, K62, C487, E507, T514 and A524.

Phylogenetic relationships of shrimp ATPα

For MP, we obtained trees with tree bisection-reconnection (TBR) branch-swapping heuristic searches in PAUP in which, all characters were equally weighted and starting trees were obtained by 1,000 random stepwise additions. Nodal support was estimated by calculation of non-parametric bootstrap (1,000 pseudo-replicates, 10 random addition replicates per pseudo-replicate) proportions (Felsenstein 1985).

Phylogenetic relationships were investigated for *L. vannamei* ATPα and other species sequences in the Protein Data Bank. One hundred and sixty nine of the 570 amino acid sequences aligned were parsimony informative. Amino acid NJ and MP trees (length=992 steps, c. i.=0.749, r. i.=0.630)

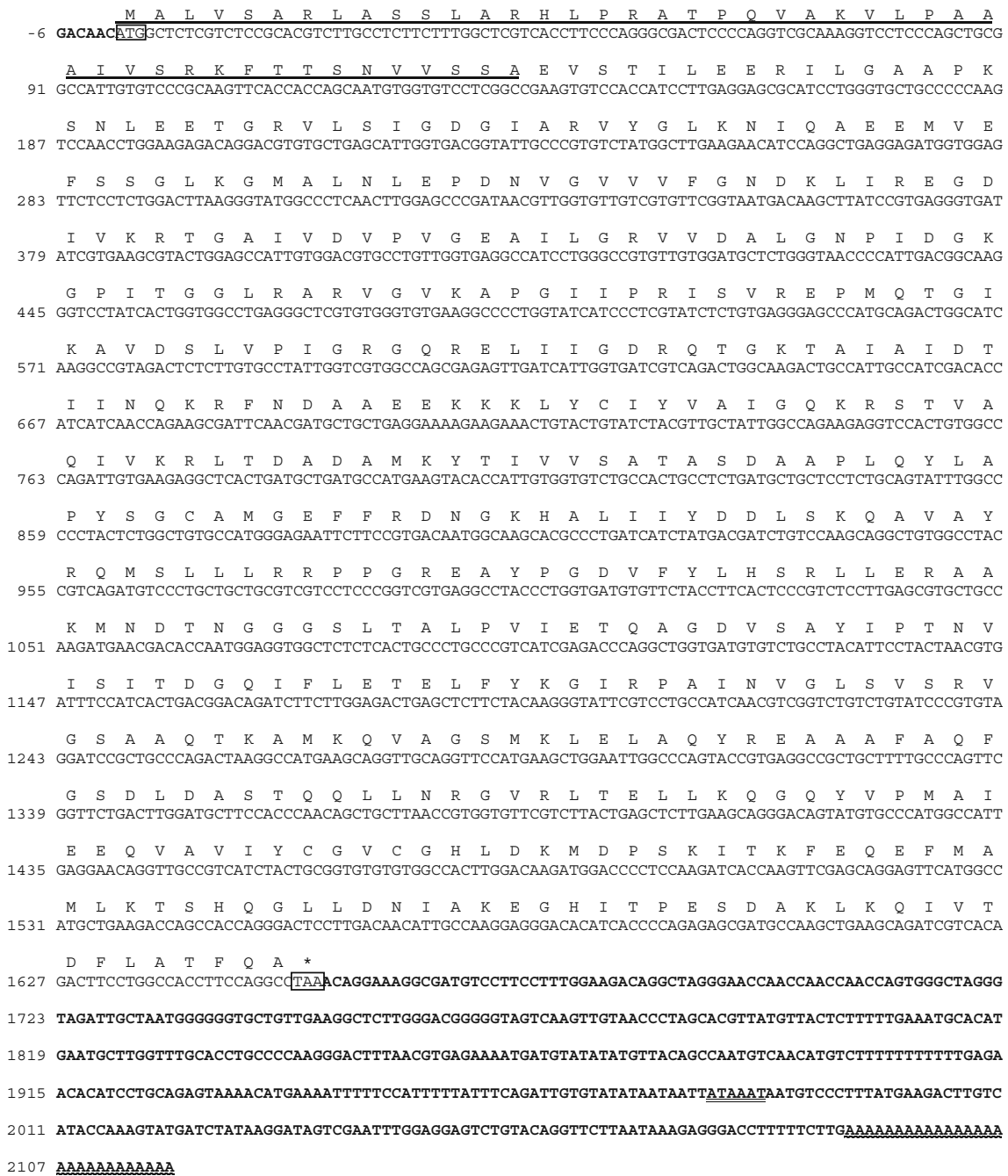


Fig. 1 Shrimp *atpα* cDNA and deduced amino acid sequences. Framed nucleotides indicate start, and stop codons. Untranslated sequence at 3' -end in bold letters; double underlined sequence

indicate the poly A signal, the poly A tail is shown at the end. Underlined amino acids at 5'-end show the signal peptide sequence

showed a similar topology for the main groups of Crustacean, Insecta and Vertebrata. Crustaceans were a close sister group of Insecta in NJ criteria, and close to Insecta + Vertebrata in MP (Fig. 3).

Atpβ cDNA sequence

The full length *atpβ* cDNA from shrimp gills (GQ848644) is 1,792 bp long. It includes a start codon

(ATG) and a stop codon (TAA) at positions 1 and 1,579, respectively. Untranslated regions were 3 bp in the 5'- end, and 211 bp in the 3'-end which included the polyadenylation signal and the poly A tail (Fig. 4). It showed an 82% identity with the *atpβ* mRNA from the crayfish *Pacifastacus leniusculus* (DQ874396), which is the only cDNA sequence that has been reported from crustaceans to date. The deduced pre-protein ATPβ is 525 amino acids long with a predicted molecular mass of 55.96 kDa and a theoretical isoelectric

Hsapiens CIYVAIGQKRSTVAQLVKRLTDADAMKYTIIVVSATASDAAPLQYLAPYSGCSMGYFRDNGKHALIIYDDLKQAVAYRQMS 325
Ccarpio CIYVAIGQKRSTVAQLVKRLTDADAMKYTIIVVSATASDAAPLQYLAPYSGCSMGYFRDNGKHALIIYDDLKQAVAYRQMS 325
Pfucata CIYVAIGQKRSTVAQIVKRLTDADAMKYTIIVVSATASDAAPLQYLAPYSGCAMGEFFRDNGMHALIIYDDLKQAVAYRQMS 325
Scerevisiae CVYVAVGQKRSTVAQLVQTEHQHDAMKYSIIVAATASEAAPLQYLAPFTAASIGEWFRDNGKHALIVYDDLKQAVAYRQLS 319
Btaurus CIYVAIGQKRSTVAQLVKRLTDADAMKYTIIVVSATASDAAPLQYLAPYSGCSMGYFRDNGKHALIIYDDLKQAVAYRQMS 325
Ecoli CIYVAIGQKASTISNVVRKLEEHGALANTIIVVATASEAALQYLARMPVALMGEYFRDRGEDALIIYDDLKQAVAYRQIS 274
 :::*** **:::*. * : .*: :::* *****:*.***** . . :* :***. * .***:*****:***:*

Lvannamei LLLRPPGREAYPGDVFYLSRLLERAAKMNDTN-----GGSLTALPVIETQAGDVSAYIPTNVISITDGGIFLE 393
Aaegypti LLLRRPPGREAYPGDVFYLSRLLERAAKMNDTN-----GGSLTALPVIETQAGDVSAYIPTNVISITDGGIFLE 394
Dmelanogas LLLRRPPGREAYPGDVFYLSRLLERAAKMSPAM-----GGSLTALPVIETQAGDVSAYIPTNVISITDGGIFLE 395
Bmori LLLRRPPGREAYPGDVFYLSRLLERAAKMSDKM-----GGSLTALPVIETQAGDVSAYIPTNVISITDGGIFLE 394
Xlaevis LLLRRPPGREAYPGDVFYLSRLLERAAKMNDHF-----GGSLTALPVIETQAGDVSAYIPTNVISITDGGIFLE 396
Ggallus LLLRRPPGREAYPGDVFYLSRLLERAAKMNSDF-----GGSLTALPAIETQAGDVSAYIPTNVISITDGGIFLE 396
Hsapiens LLLRRPPGREAYPGDVFYLSRLLERAAKMNDAF-----GGSLTALPVIETQAGDVSAYIPTNVISITDGGIFLE 396
Ccarpio LLLRRPPGREAYPGDVFYLSRLLERAAKMNSDF-----GGSLTALPVIETQAGDVSAYIPTNVISITDGGIFLE 396
Pfucata LLLRRPPGREAYPGDVFYLSRLLERAAKMNDN-----GGSLTALPVIETQAGDVSAYIPTNVISITDGGIFLE 396
Scerevisiae LLLRRPPGREAYPGDVFYLHPRLLEERAALKESE-----GGSLTALPVIETQAGDVSAYIPTNVISITDGGIFLE 390
Btaurus LLLRRPPGREAYPGDVFYLSRLLERAAKMNDAF-----GGSLTALPVIETQAGDVSAYIPTNVISITDGGIFLE 396
Ecoli LLLRRPPGREAYPGDVFYLSRLLERAAKMNDAF-----GGSLTALPVIETQAGDVSAYIPTNVISITDGGIFLE 356
 *****:*****.*****:;. ***** ***.*****:*****:*****

ATP-synt_ab_C

Lvannamei TELFYKIRPAINVGLSVSRVGSAAQTKAMKQVAGSMKLELAQYREAAFAQFGSDLDASTQOLLNRGVRLELLKQGYVP 475
Aaegypti TELFYKIRPAINVGLSVSRVGSAAQTKAMKQVAGSMKLELAQYREAAFAQFGSDLDAAATQOLLNRGVRLELLKQGYVP 476
Dmelanogas TELFYKIRPAINVGLSVSRVGSAAQTKAMKQVAGSMKLELAQYREAAFAQFGSDLDAAATQOLLNRGVRLELLKQGYVP 477
Bmori TELFYKIRPAINVGLSVSRVGSAAQTKAMKQVAGSMKLELAQYREAAFAQFGSDLDAAATQOLLNRGVRLELLKQGYVP 476
Xlaevis TELFYKIRPAINVGLSVSRVGSAAQTRAMKQVAGTMKLELAQYREAAFAQFGSDLDAAATQOLLNRGVRLELLKQGYVP 478
Ggallus TELFYKIRPAINVGLSVSRVGSAAQTRAMKQVAGTMKLELAQYREAAFAQFGSDLDAAATQOLLNRGVRLELLKQGYVP 478
Hsapiens TELFYKIRPAINVGLSVSRVGSAAQTRAMKQVAGTMKLELAQYREAAFAQFGSDLDAAATQOLLNRGVRLELLKQGYSP 478
Ccarpio TELFYKIRPAINVGLSVSRVGSAAQTRAMKQVAGTMKLELAQYREAAFAQFGSDLDAAATQOLLNRGVRLELLKQGYSP 478
Pfucata TELFYKIRPAINVGLSVSRVGSAAQTKAMKQVAGSMKLELAQYREAAFAQFGSDLDQATQOLLNRGVRLELLKQGYVP 478
Scerevisiae AELFYKIRPAINVGLSVSRVGSAAQVKALKQVAGSLKFLAQYREAAFAQFGSDLDASTKQTLVGRERLTQLLKQNYSP 472
Btaurus TELFYKIRPAINVGLSVSRVGSAAQTRAMKQVAGTMKLELAQYREAAFAQFGSDLDAAATQOLLNRGVRLELLKQGYSP 478
Ecoli TNLFNAGIRPAVNPGISVSRVGSAAQTKIMKLSGGIRTAQYRELAASFQFASDLDATRNQLDHGQVTELLKQGYAP 438
 ::* *::*:*** *::*:***.***: :*:*** :* ***** ***.***** :*: * * :*:*** ** *

Lvannamei MAIEEQVAVIYCGVCGHLDKMDPSKITKFEQEFMAMLKTSHQGLLDNIAKEGHITPESDAKLKQIVTDFLATFQA-- 550
Aaegypti MAIEEQVAVIYCGVRYLDKMDPSKITAFEREFFLAHVKTEKALLSQIATDGKISDETEAKLKNVVSFMSFSG-- 551
Dmelanogas MAIEDQVAVIYCGVGRHLDKMDPAKITKFEKEFLOHIKTSQALLDTIAKDGAISEASDAKLKDIVAKFMSFQ-- 552
Bmori MAIEEQVAVIYCGVGRHLDKMDPSKITAFEREFLOHIKTSHQGLLDNIAKDGQITPESDASLKKIVTDFLATFTQSQ 553
Xlaevis MAIEEQVAVIYAGVGRHLDKMDPSKITKPEAFLAHVKSQHQLLSTIRTEGKISDQTEAKLKEIVNFLSTFEA-- 553
Ggallus MAIEEQVAVIYAGVGRHLDKMDPSKITKPEAFLAHVKSQHQLLSTIRTEGKISDQTEAKLKEIVNFLSTFEA-- 553
Hsapiens MAIEEQVAVIYAGVGRHLDKMDPSKITKPEAFLAHVKSQHQLLSTIRTEGKISDQTEAKLKEIVNFLSTFEA-- 553
Ccarpio MAIEEQVAVINAGVGRHLDKMDPSKITKPEAFLAHVKSQHQLLSTIRTEGKISDQTEAKLKEIVNFLSTFEA-- 552
Pfucata MAIEEQVAVIYAGVGRHLDKMDPSKITKPEAFVSHIRGSQQLLSTIRTEGKISDQTEAKLKEIVNFLSTFEA-- 553
Scerevisiae LATEEQVPLIYAGVNGHLDGIELSRIGEFESSFLSYLKNHNEELLEIREKELSKELLASLKSATESFVATF--- 545
Btaurus MAIEEQVAVIYAGVGRHLDKMDPSKITKPEAFLAHVKSQHQLLSTIRTEGKISDQTEAKLKEIVNFLSTFEA-- 553
Ecoli MSVAQQSLVLPFAAERGLADVELSKIGSFEAALLAYVDRDHAPLMQEIQTGGYNDIEGKLGKILDSFKATQSW-- 513
 : : * : : . . * : : : * * : : . . * : * * * : *

Fig. 2 (continued)

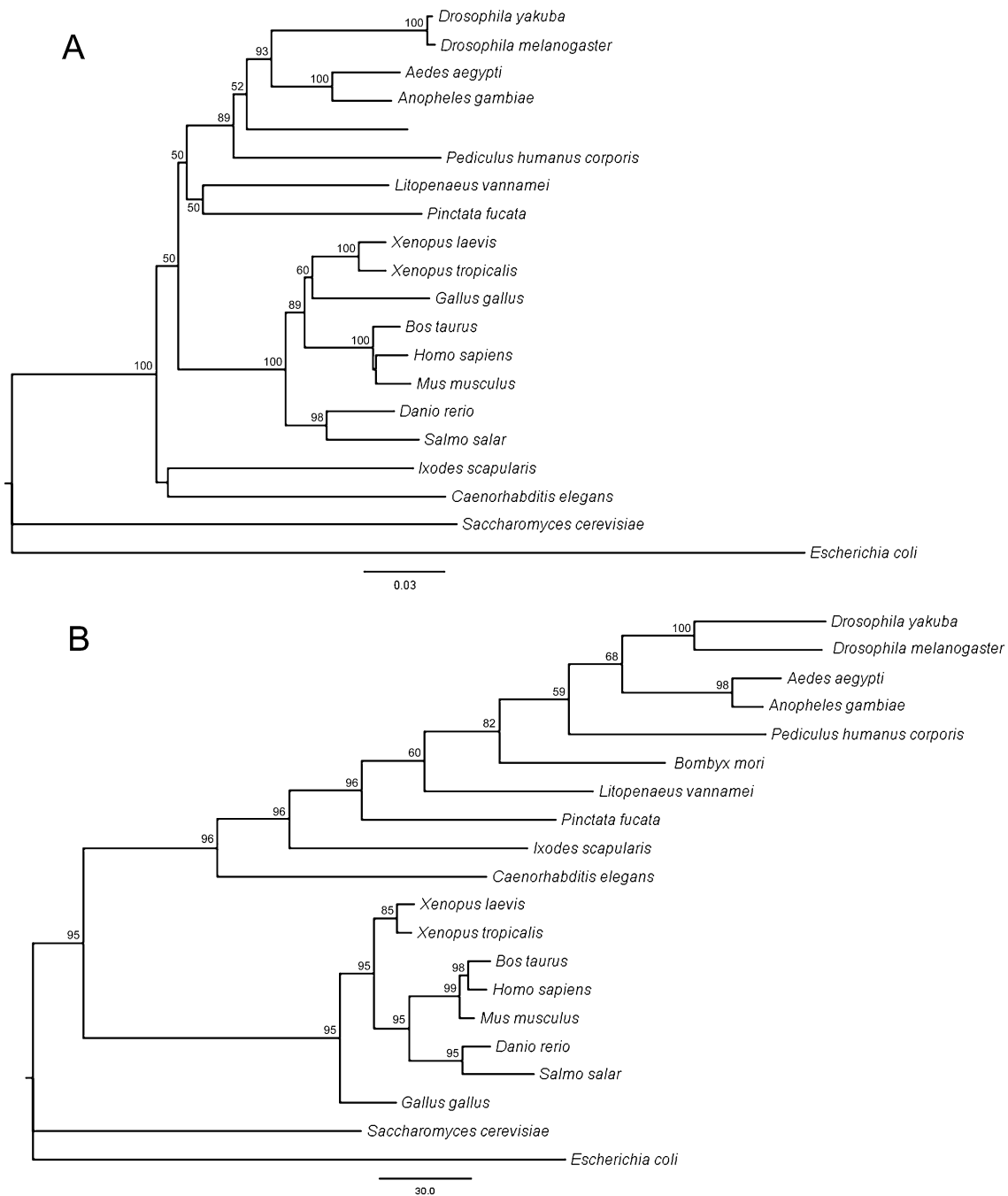


Fig. 3 Topology of phylogenetic trees recovered using neighbor joining (**a**), and maximum parsimony (**b**) from amino acid sequences of the white shrimp ATP α . Numbers above the nodes represent nonparametric bootstrap percentages

point of 5.03. The putative signal peptide contains 43 amino acids, 6 positively charged and no negatively charged residues as observed in the signal peptide of the ATP α subunit (Fig. 4). The mature protein comprises 482 amino acids, a predicted molecular mass of 51.45 kDa and an isoelectric point of 4.78.

The three conserved domains from the ATP β protein were identified in this sequence as: (i) ATP-synt_{ab}_N domain which includes residues 59–126, (ii) the ATP-synt_{ab} domain between residues 182–402 containing the

Walker A motif (GGAGVGKT), which forms a P-loop responsible for triphosphate binding at positions 203–210, and five residues (LLFID) that were identified as the Walker B motif at positions 299–303; the third domain, ATP-synt_{ab}_C was found at positions 415–525 (Fig. 5). Additional conserved sequences were found in shrimp ATP β as DELSEED which includes residues 441–447, and forms a negatively charged loop near to the site where the IF₁ inhibitor, which regulates the hydrolytic activity of the


```

      M L G A A O R A C S T I L K A A K P A V V S K G L O N V G
-3  ATCATGTTGGGAGCTGCACAGCGCTTGCTCCACCATCCTAAAGGCAGCGAAGCCTGCTGCTCTCCAAGGGCCTGCAAATGTAGGC
      S K T L P A L Y T C O R N Y A A K A E A A T Q T G V A N G S
91  TCCAAGACTCTTCCAGCGCTCTACACCTGCCAGCGCAACTATGCTGCCAAGGCTGAGGCTGCCACCCAGACTGGTGTGGCCAATGGCAGT
      V V A V I G A V V D V Q F D G E L P P I L N A L E V A N R S
181 GTAGTAGCTGTCAATGGTGTGTGGTGGACGTCCAGTTCGATGGAGAGCTCCCCCTATTCTCAATGCTCTTGAGGTTGCCAACCGCTCC
      P R L V L E V A Q H L G E N T V R T I A M D G T E G L I R G
271 CCAAGGCTGGTGTGTGAGGTTGCTCAGCATCTTGGTGAGAACTGTCCGCACCATTTGCTATGGATGGTACTGAGGGTCTCATCCGTGGT
      N A V V D T G S P I S I P V G P G T L G R I I N V I G E P I
361 AATGCTGTCTGTGACTGGAAGCCCATCTCCATCCCTGGTCTGGTACTCTTGGCCGATTATCAATGTGATTGGTGAGCCCAT
      D E R G P I P T E H F S A I H A E A P D F V E M S V E Q E I
451 GATGAACGTGGCCCATTCCTCACTGAACACTTCTCTGCTATTATGCTGAGGCTCCCGACTTCGTTGAGATGTCTGTGAGCAGGAGATT
      L V T G I K V V D L L A P Y S K G G K I G L F G G A G V G K
541 CTCGTAACCTGGCATCAAGGTGGTCGACCTCTTGGCCCCATACTCCAAGGGAGGAAAGATTGGTCTGTTTCGGTGGTGTGGTGTAGGAAAG
      T V L I M E L I N N V A K A H G G Y S V F A G V G E R T R E
631 ACTGTACTTATCATGGAAGTATTAACAACGTTGCCAAGGCTCACGGTGGTACTCAGTATTTGCTGGTGTGGGAGAGCGCACCCGTGAG
      G N D L Y H E M I E S G V I S L K D D T S K V S L V Y G Q M
721 GGTAAACGATCTGTACCAGAGATGATTGAGTCTGGTGTCTCTCTGAAGGATGATACTCCAAGGATCTCTCGTGTACGGTACAGATG
      N E P P G A R A R V A L T G L T V A E Y F R D Q E G Q D V L
811 AACGAGCCCCAGGTGCCCGTCCCGTGTGCGCCCTGACTGGTCTGACTGTGGCCGAGTACTTCCGTGATCAGGAAGGTCAAGATGTGCTG
      L F I D N I F R F T Q A G S E V S A L L G R I P S A V G Y Q
901 CTCTTCATTGACAAATTTTCCGCTTCACACAAGCTGGTTCGAGGTGTCTGCCCTGCTGGGTCGTATCCCATCTGCTGTAGGTTACCAG
      P T L A T D M G S M Q E R I T T T K K G S I T S V Q A I Y V
991 CCTACTCTGGCCACTGACATGGGTAGCATGCAGGAAAGAATTACTACCACCAAGAAGGATCAATTACCTCTGTGCAGGCCATCTATGTA
      P A D D L T D P A P A T T F A H L D A T T V L S R G I A E L
1081 CCTGCTGATGACTTGACTGATCCTGCCCCAGCCACCATCTCGCTCACTTGGACGCTACTACTGTGTGTCTCGTGGTATTGCCGAGTTG
      G I Y P A V D P L D S I S R I M D A N I I G H E H Y N V A R
1171 GGTATTTACCTGCTGTGGATCCTCTCGATTCCATCTCCGATCATGGACGCCAACATCATCGGACACGAACATTACAATGTTGCCCGT
      S V Q K I L Q D H K S L Q D I I A I L G M D E L S E E D K L
1261 AGTGTGCAGAAGATTCTTCAGGATCATAAGTCGCTCCAGGATATATGCTATCTTGGGTATGGATGAATTGTCTGAGGAGGACAAGCTC
      T V A R A R K I Q K F L S Q P F Q V A E V F T G Y S G K F V
1351 ACAGTCGCCCGTGCACGTAAGATCCAGAAGTTCTGTGCAGCCTTTCCAAGTGGCTGAGGTTTACTGGCTACTCTGAAAGTTCGTT
      S L P D P I R S F K E I L A G K Y D D L P E A P F Y M Q G S
1441 TCCCTGCCCTGATCCCATCAGGAGCTTCAAGGAAATCTGGCTGGCAAGTACGATGACCTCCCTGAAGCTCCCTTCTACATGCAAGGAAGT
      I E D V I E K A E Q L A A Q P S *
1531 ATTGAGGATGTCAATGAAAAGGCAGAACAGTTGGCTGCCAGCCCAGCTAAGGAGGAAATATAAATTTGGGGTATTTTAAACATGTGTACA
1621 GGGCTCTGGAAGAAATATCCATGTTCTCTTTGTTGCAAGTAAGGGCCAAGTGGTCTGTTCTTAGACTATGGCAAACAATATTTTAG
1711 GGGTACTCCGAGAATCTGGAGTAACTTCTGTTGTACAGAATTCCAGTGATAATGTAATTTATATAAATAATCCAGAAACCCAAAAA
1801 AAAAAAAAAAAAAAAAAAAAAAAA
    
```

Fig. 4 Shrimp *atpβ* cDNA and deduced amino acid sequences. Framed nucleotides indicate start, and stop codons. Untranslated sequences at 5'- and 3'-ends in bold letters; double underlined

sequence indicate the poly A signal, the poly A tail is shown at the end. Underlined amino acids at 5'-end show the signal peptide sequence

F₀F₁ ATP-synthase, interacts with the enzyme (Cabezon et al. 2001). The GERXXE sequence was detected at positions 234–239, this is suggested to play a role in the process of ATP hydrolysis by interacting with subunit alpha at the catalytic site (Wada et al. 2000; Fig. 5).

Eleven ATP binding sites were detected along the ATPβ protein at positions 206, 209, 210, 211, 235, 236, 239, 303, 307, 392, and 393, all of them are highly conserved between eukaryotes. Thirty nine sites were located at the interface with

ATPβ subunit at positions: 151, 168, 170, 171, 173, 175, 236–238, 241, 269–271, 276, 307, 310, 314, 320–322, 324, 325, 330, 334, 341, 358, 361, 362, 366, 373, 375–377, 388, 389, 398, 399, 401, and 403. Along the ATPβ we identified amino acid substitutions shared only by crustacean species as *P. leniusculus*, and *L. vannamei* at specific sites as G74, E75, N120, S130, G136, E158, S161, D169, S194, D258, S263, I401, H428, S487, E490, and P503. Some other substitutions as S59, A86, I117, V123, H159, A407, H412, S420, P482,

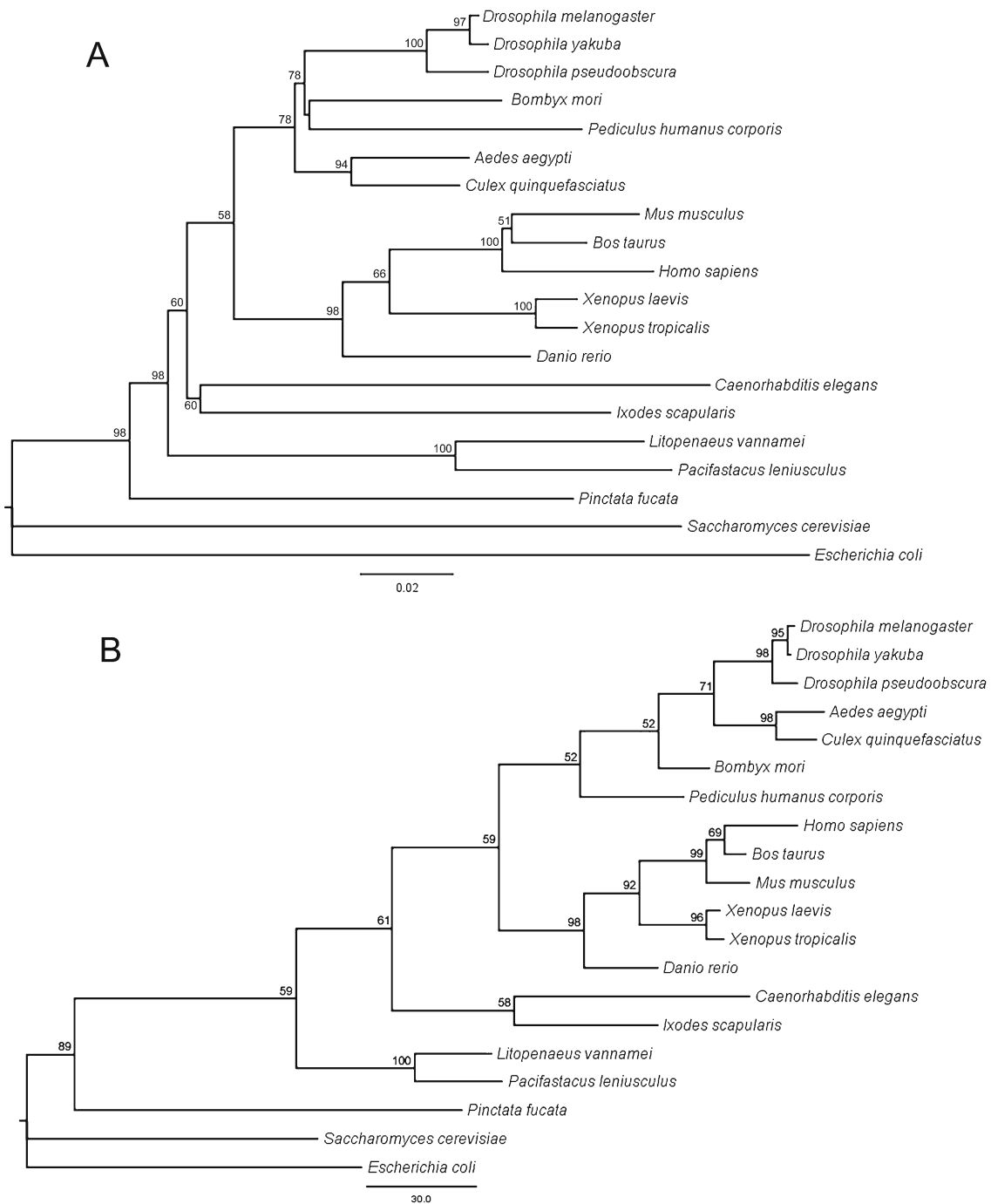


Fig. 6 Topology of phylogenetic trees recovered using neighbor joining (**a**), and maximum parsimony (**b**) from amino acid sequences of the white shrimp ATP β . Numbers above the nodes represent nonparametric bootstrap percentages

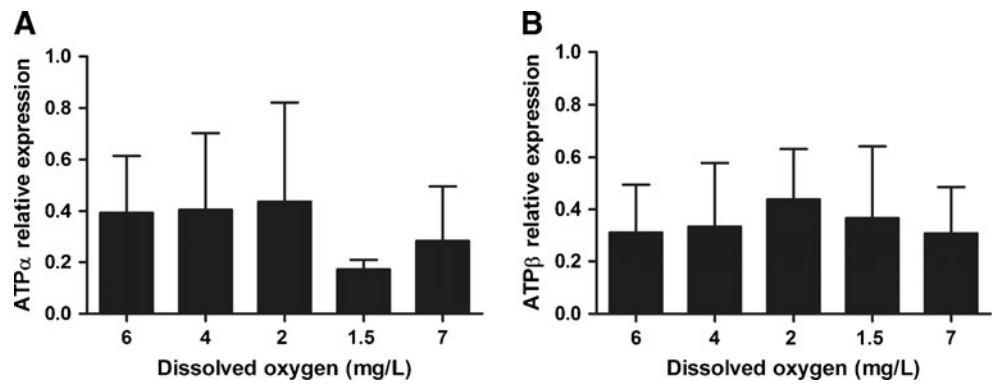
shrimp subunits and/or other ATP-synthase subunits (Muhlia-Almazan et al. 2008).

Although mRNA isoforms have been described for bovine and human (Pierce et al. 1992), we did not find differences between analysed sequences from different shrimp tissues, neither for *atp α* transcripts, nor for *atp β* (data not shown), suggesting that no additional mRNA isoforms are synthesized from genes encoding the mRNAs characterized in this

study; however the possibility of additional genes encoding other transcripts for both *atp α* and *atp β* already exists.

Analyses showed that the shrimp deduced proteins of ATP α and ATP β subunits are highly conserved, both containing the three major domains, the two Walker motifs and specific ATP-binding sites characterizing these proteins (Walker and Runswick 1983; Walker et al. 1989; Abrahams et al. 1994; Atteia et al. 1997), and some other above

Fig. 7 Relative expression of **A** *atp α* , and **B** *atp β* transcripts in the gills of shrimp at different oxygen concentrations. Data represent the mean and standard deviation value



mentioned elements that allow them to integrate the water-soluble F_1 motor that forms the catalytic portion of the enzyme (Von Ballmoos et al. 2009). Our results are in agreement with the current paradigm that the central role of these proteins in ATP synthesis is due to subtle interactions among subunits, which are only possible by complex complementarities. Hence selective pressure must punish mutants and what we see is highly conserved proteins (Peña et al. 1995).

In addition to conserved characteristics, we detected unique elements in the amino acid sequences of the N-terminal signal peptides of both shrimp subunits when compared with other species. The signal peptide of shrimp ATP α subunit shares length and gaps with those from insect species (residues 46 to 48; Peña et al. 1995); signal peptides from vertebrate species are usually 49 residues long and show different conserved residues (Walker et al. 1985). The shrimp ATP β signal peptide sequence showed no identity with invertebrate or vertebrate species; however, it showed a high identity percentage, 82%, when compared to that of the crayfish *P. leniusculus* sharing length and gaps, thus both crustacean sequences were different from those of other invertebrate and vertebrate species. These results are in agreement with knowledge indicating that the signal peptide of mitochondrial proteins is highly variable, both in length and sequence, and that conserved elements are limited to their basic character and secondary structure (Hendrick et al. 1989). The predicted molecular weight of both shrimp ATP-synthase subunits also differed when compared to other taxa groups. The ATP α subunit is highly conserved in molecular mass among

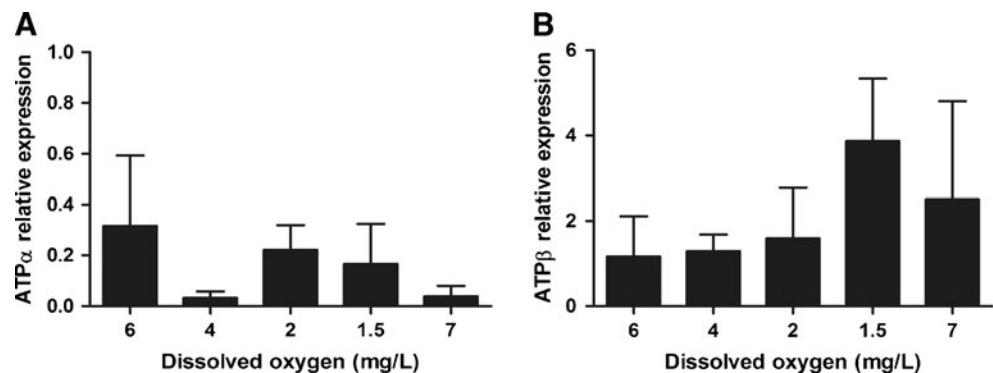
species, but ATP β is larger than those proteins from other invertebrates and similar to those from vertebrates.

The results of phylogenetics based upon MP and ML analyses of the nucleotide and amino acid sequences provided similar basic topology branch support by both criteria, as the general topology of the trees shown in the entire analysis. Higher values were obtained for amino acid than for nucleotide trees due to the presence of synonymous codons. Genetic distances and parsimony bootstrap showed strong statistical bootstrap support for the association of *L. vannamei* to Insecta and Vertebrata clade. NJ ATP α showed monophyly to Insecta, but MP moves monophyly to a lower branch including Nematoda and Protist. This information confirms our previous observations about this subunit.

The ATP β sequences were more reliable showing the clade of crustaceans as a sister of all the Insecta, Vertebrata and isolated from Nematode and Protist. NJ and MP of ATP β showed monophyly to a main group of Insecta and Vertebrata fixing the monophyly to a lower branch close to Mollusca and constructing a big clade. ATP β were more consistent in showing the phylogentic relationships in a broad scale as a result of the conservation of the sequences. Conservation of both units may not be an artifact to conclude the relationships of the main clades in this study given the limited number of taxa whose data were available to be included in this research.

Unique characteristics found in shrimp proteins ATP α and ATP β in this research should be deeply analyzed since some of these registered substitutions could be related to specific enzymatic properties of the soluble F_1 -ATP

Fig. 8 Relative expression of **A** *atp α* , and **B** *atp β* transcripts in the pleopods of shrimp at different oxygen concentrations. Data represent the mean and standard deviation value



synthase portion, as reported by Li and Neufeld (2001), after they isolated and characterized this portion from the gills of the crayfish *Orconectes virilis*. They emphasized the high ATPase activity of the enzyme, as well as sensitivities to inhibitors and modulators that distinguish the crustacean enzyme from all those previously examined. As observed in figures, crustacean proteins can share specific amino acid substitutions with microbial, vertebrate and invertebrate species, suggesting these species as interesting models to study.

Crustaceans exposed to hypoxia biochemical compensation evolve as a complex and highly integrated series of responses to maintain cellular homeostasis by adjusting various metabolic pathways, where ATP synthesis/hydrolysis is crucial (McMahon 2001). The exposure to oxygen depleted water increases ventilation frequency since gills O₂ diffusion is affected (Morris and Callaghan 1998), implying an increase in the energy demand of shrimp. In addition, studies state that a reduction in metabolism is a manner of avoiding anaerobiosis (Hochachka 1988). However, as hypoxia continues, shrimp produce lactate as the end product of anaerobic metabolism, and the concentration of cellular ATP decreases. All these physiological responses agree with those observed in our experimental shrimp exposed to increasing degrees of hypoxia, confirming the hypoxia-compensating status along the assay.

No coordinated changes were detected in the mRNA amounts of these two nucleus-encoded subunits along the assay. Previously, the presence of coordinated mechanisms was reported when comparing the nuclear and mitochondrial subunits of the enzyme (Muhlia-Almazan et al. 2008); however, it seems not to be the case between nuclear subunits from both evaluated tissues.

Concerning the relative expression of *atpβ* in shrimp pleopods, an up-regulation of 3-fold was observed in the lowest OC (1.5 mg/L). This increase was also observed for *atp6* and *atp9* mRNAs of shrimp at hypoxia in the digestive gland (Martinez-Cruz 2007); this observation supports the suggestion that the expression of the nuclear *atpβ* subunit is strictly coordinated with the expression of *atp6* (Peña et al. 1995), which is a mitochondrially encoded subunit in the fruit fly *D. melanogaster*. In the grass shrimp, *Palaemonetes pugio*, exposed to 1.5 mg/L OC for 3 days, an increase in the *atpf* mRNA concentration was detected and, in agreement with our results, this increase was not coordinated since no changes were detected in the mRNA concentration of both nuclear *atpβ* and *atpd* subunits (Brown-Peterson et al. 2008).

The increase of *atpβ* mRNAs in pleopods during hypoxia, and the subsequent decrease as response to normoxia during re-oxygenation agrees with our previous observations (Martinez-Cruz 2007). These changes are explained as a response to a decreasing OC of water by synthesizing new ATP-synthase complexes in the early phase of hypoxia, in order to maintain the mitochondrial

membrane potential by using the still available intracellular ATP molecules. Then, after oxidative phosphorylation is reduced or absent, and the accumulation of lactate reduces tissues pH, ATP-synthases will change from ATP producers to powerful ATP consumers as observed in the ischemic myocardium of vertebrates (Di Lisa et al. 1998).

We propose that the increasing amount of mRNAs in response to hypoxia, and the existence of coordinated mechanisms of gene's expression, as we previously reported in shrimp (Muhlia-Almazan et al. 2008) are tissue-specific responses. Each of these responses are tightly related to tissues function since gills in this research, and muscle in the previous report (Martinez-Cruz 2007) were not affected by the oxygen reduction, and no coordinated expression was observed in this report between nuclear encoded genes of the ATP-synthase subunits.

Previous studies in shrimp confirm our proposal by demonstrating that the genes expression profile of a tissue is tightly related to its function (Clavero-Salas et al. 2007). To date, the amount of mRNA of some of the ATP-synthase subunits from crustaceans and other marine invertebrates have been reported to be affected by factors as viral infections, osmotic stress and hypoxia in different tissues as the midgut gland, gills, and hemocytes, which affects their primary role (De la Vega et al. 2007; Zhao et al. 2007; Soñanez-Organis et al. 2009).

The results of this study suggest that changes in the amount of mRNAs encoding the F₀F₁ ATP-synthase subunits are part of the mechanisms allowing shrimp to deal with metabolic adjustment to tolerate hypoxia. This new information about mitochondrial enzymes from marine invertebrates as crustaceans not only confirms predictable elements about the catalytic subunits of the ATP synthase, but also allowed us to detect those species-specific characters that could explain organism adaptive features to their aquatic environment. Future studies should be addressed to deeply analyse a predictive model of the F₁ portion of shrimp ATP synthase. The isolation and characterization of the subcomplex and its forming parts, and ATPase kinetics will help to understand and explain shrimp enzyme differences.

Acknowledgments AMA acknowledges support from Consejo Nacional de Ciencia y Tecnología (CONACYT National Council for Research and Technology, Mexico) for grant J48989-Z. OMC and ARR thank CONACYT for a graduate scholarship. We also thank Dr. Arturo Sanchez-Paz for critical reading of this manuscript.

References

- Abrahams J, Leslie A, Lutter R, Walker J (1994) Nature 370:621–628
- Alberts B, Johnson A, Lewis J, Raff M, Roberts K, Walter P (2008) Molecular biology of the cell, garland science. Taylor & Francis Group, New York

- Altschul SF, Madden TL, Schäffer AA, Zhang J, Zhang Z, Miller W, Lipman DJ (1997) *Nucleic Acids Res* 25:3389–3402
- Atteia A, Dreyfus G, Gonzalez-Halphen D (1997) *Biochim Biophys Acta* 1320:275–284
- Boyer PD (1997) *Ann Rev Biochem* 66:717–749
- Breen G (1988) *Biochem Biophys Res Commun* 152:264–269
- Brown-Peterson N, Manning S, Patel V, Denslow N, Brouwer M (2008) *Biol Bull* 214:6–16
- Cabezón E, Runswick MJ, Leslie AGW, Walker JE (2001) *EMBO J* 20(24):6990–6996
- Chan S, Rankin S, Keeley L (1988) *Biol Bull* 175:185–192
- Claros M, Vincens P (1995) *Eur J Biochem* 241:770–786
- Clavero-Salas A, Sotelo-Mundo R, Gollas-Galvan T, Hernandez-Lopez J, Peregrino-Uriarte A, Muhlia-Almazan A, Yepiz-Plascencia G (2007) *Fish Shellfish Immunol* 23:459–472
- De la Vega E, Hall MR, Wilson KJ, Reverter A, Woods RG, Degnan BM (2007) *Physiol Genomics* 31:126–138
- Di Lisa F, Menabo R, Canton M, Petronilli V (1998) *Biochim Biophys Acta* 1366:69–78
- Felsenstein J (1985) *Evolution* 39:783–791
- Gross P, Bartlett T, Browdy C, Chapman R, Warr G (2001) *Dev Comp Immunol* 25:565–577
- Hendrick JP, Hodges PE, Rosenberg LE (1989) *Proc Natl Acad Sci USA* 86:4056–4060
- Hochachka PW (1988) *Can J Zool* 66:152–158
- Hoskins RA, Carlson JW, Kennedy C, Acevedo D, Evans-Holm M, Frise E, Wan KH, Park S, Mendez-Lago M, Rossi F, Villasante A, Dimitri P, Karpen GH, Celniker SE (2007) *Science* 316:1625–1628
- Hüttemann M, Lee I, Pecinova A, Pecina P, Przyklenk K, Doan J (2008) *J Bioenerg Biomembr* 40:444–456
- Kataoka H, Biswas C (1991) *Biochim Biophys Acta* 1089:393–395
- Lalanne E, Mathieu C, Vedel F, De Paepe R (1998) *Plant Mol Biol* 38:885–888
- Li Z, Neufeld GJ (2001) *Comp Biochem Physiol* 128B:325–338
- Livak KJ, Schmittgen TD (2001) *Methods* 25:402–408
- Marchler-Bauer A, Anderson JB, Chitsaz F, Derbyshire MK, DeWeese-Scott C, Fong JH, Geer LY, Geer RC, Gonzales NR, Gwadz M, He S, Hurwitz DI, Jackson JD, Ke Z, Lanczycki CJ, Liebert CA, Liu C, Lu F, Lu S, Marchler GH, Mullokandov M, Song JS, Tasneem A, Thanki N, Yamashita RA, Zhang D, Zhang N, Bryant SH (2009) *Nucleic Acids Res* 38:D205–D210
- Martinez-Cruz O (2007) Expresion genica de las subunidades *atp6* mitocondrial y *atp6* nuclear del complejo ATP-sintasa en el camaron blanco *Litopenaeus vannamei* en condiciones de hipoxia. Masters thesis. Centro de Investigacion en Alimentacion y Desarrollo, A.C. Sonora, Mexico
- McMahon B (2001) *Respir Physiol* 128:349–364
- Morris S, Callaghan J (1998) *J Comp Physiol* 168B:377–388
- Morris S, Aardt W, Ahern M (2005) *Aquat Toxicol* 75:16–31
- Muhlia-Almazan A, Martinez-Cruz O, Navarrete del Toro M, Garcia-Carreño F, Arreola R, Sotelo-Mundo R, Yepiz-Plascencia G (2008) *J Bioenerg Biomembr* 40:359–369
- Pedersen P (2007) *J Bioenerg Biomembr* 39:349–355
- Peña P, Ugalde C, Calleja M, Garesse R (1995) *Biochem J* 312:887–897
- Pierce DJ, Jordan EM, Breen GAM (1992) *Biochim Biophys Acta* 1132:265–275
- Ribeiro JM, Arca B, Lombardo F, Calvo E, Phan VM, Chandra PK, Wikel SK (2007) *BMC Genomics* 8:6
- Sambrook J, Russell DW (2001) *Molecular cloning: a laboratory manual*. Cold Spring Harbor, New York
- Schatz G, Butow RA (1983) *Cell* 32:316–318
- Soñanez-Organis J, Peregrino-Uriarte A, Gomez-Jimenez S, Lopez-Zavala A, Forman HJ, Yepiz-Plascencia G (2009) *Comp Biochem Physiol* 150C:395–405
- Thompson JD, Higgins DG, Gibson TJ (1994) *Nucleic Acids Res* 22:4673–4680
- Vargas-Albores F, Guzman-Murillo MA, Ochoa JL (1993) *Comp Biochem Physiol* 106A:299–303
- Von Ballmoos C, Wiedenmann A, Dimroth P (2009) *Annu Rev Biochem* 78:649–672
- Wada Y, Sambongi Y, Futai M (2000) *Biochim Biophys Acta* 1459:499–505
- Walker J, Runswick M (1983) *J Biol Chem* 258:3081–3089
- Walker J, Saraste M, Runswick M, Gay N (1982) *EMBO J* 8:945–951
- Walker J, Fearnley I, Gay N, Gibson B, Northrop F, Powell S, Runswick M, Sarate M, Tybulewicz V (1985) *J Mol Biol* 184:677–701
- Walker J, Powell S, Viñas O, Runswick M (1989) *Biochemistry* 28:4702–4708
- Walker J, Lutter R, Dupuis A, Runswick M (1991) *Biochemistry* 30:5369–5378
- Wu R, Lam P, Wan K (2002) *Environ Pollut* 118:351–355
- Zhao ZY, Yin ZX, Weng SP, Guan HJ, Li SD, Xing K, Chan SC, He JG (2007) *Fish Shellfish Immunol* 22:520–534